CLOCK evolved in cnidaria to synchronize internal rhythms with circadian environmental cues

Mieka Rinsky[1†*], Raphael Aguillon[1,2†*], Noa Simon-Blecher[1], Tirza Doniger[1], Lior Appelbaum[1,2], Oren Levy[1*]

[1]Mina and Everard Goodman Faculty of Life Sciences, Bar-Ilan University, Ramat Gan 52900, Israel.

[2]The Multidisciplinary Brain Research Center, Bar-Ilan University, Ramat Gan 52900, Israel

[†]These authors contributed equally to this work

*Corresponding authors: Mieka Rinsky miekari9@gmail.com, Raphael Aguillon raphael.aguillon@outlook.fr and Oren Levy oren.levy@biu.ac.il

Abstract

The circadian clock enables anticipation of the day/night cycle in animals ranging from cnidarians to mammals. Circadian rhythms are generated through a transcription-translation feedback loop (TTFL) involving negative and positive factors. CLOCK is a central conserved positive factor in the animal kingdom. However, the functional evolutionary origin and mechanism of action of CLOCK in basal animals are unknown. In cnidarians, the transcription of putative core clock genes, including *Clock*, is arrhythmic under constant conditions, and it is unclear how the TTFL model can regulate physiological rhythms. Here, we used the CRISPR/Cas9 system to generate a *Clock* mutant (*Clock*$^{-/-}$) in *Nematostella vectensis*. High-throughput video tracking of locomotor activity in *Clock*$^{-/-}$ adults revealed that light regulates rhythmic behavior, while CLOCK maintains a 24-hour circadian rhythm under constant light conditions, and even under a 6-hour cycle, reminiscent of the tidal rhythm. Transcriptome profiling identified hundreds of differentially expressed genes in *Clock*$^{-/-}$ adults, particularly genes involved in cell cycle and neural development. In accordance with the rhythmic behavioral profile, computational analysis revealed rhythmic and arrhythmic gene expression in wild-type and *Clock*$^{-/-}$ adults, respectively, under constant dark conditions. Notably, hierarchal light- and *Clock*-signaling is required to drive rhythmic transcription of the core clock genes. These findings demonstrate that CLOCK has evolved in cnidarians to maintain synchronized 24-hour rhythmic physiology and behavior despite the chaotic inputs of environmental cues.

Introduction

Throughout the history of life on Earth, organisms have had to adapt to a constantly changing environment, including the ~24-hour daily rhythm of light/dark, driving the development of endogenous biological clocks. The circadian clock, which is entrained by external stimuli such as light, enables the organism to anticipate the onset of the light and dark phases and synchronize its physiology and behavior in harmony with the environment. This, in turn, enhances the organism's fitness and survival[1–3]. From single-celled organisms to metazoans, circadian clocks have evolved multiple times, highlighting their importance to living organisms[1,2]. Despite the fundamental role circadian clocks play in regulating the biorhythmicity of living organisms, their evolutionary origin and intricate molecular mechanisms remain ambiguous in early diverging animal lineages, such as cnidaria.

Rhythmic phenomena, including calcification, reproduction, and diel behavior patterns, have been examined in cnidarian species[3–8]. While some of these patterns were found to be directly triggered by environmental stimuli, such as light, others persist in the absence of external cues, suggesting the presence of an internally generated and self-sustaining circadian clock[6,9,10]. At the molecular level, cnidarians possess homologs of putative core clock genes found in bilaterians[11–13]. Several studies have shown that most of these genes display diel expression patterns under light/dark cycles. However, in contrast to most animals, their oscillation generally ceases without the presence of light cues[14–16]. Thus, how the core clock genes orchestrate rhythmic gene expression and circadian behaviors in cnidarians remains unclear.

One of the most studied cnidarian species in the field of chronobiology is the estuarine sea anemone, *Nematostella vectensis*. Few studies have shown that in diel lighting, the locomotor behavior of *N. vectensis* has a ~24-h rhythm that is maintained under constant conditions suggesting it is regulated by an endogenous circadian clock[6,17–19]. In accordance, the *N. vectensis* genome codes for conserved core clock genes such as *Clock*, *Cycle*, *Timeout*, and the cryptochromes *Cry1a* and *Cry1b*[12,13]. The proposed circadian clock model in *N. vectensis* is composed of the positive transcription factors, CLOCK and CYCLE, that heterodimerize and upregulate light-dependent cryptochrome genes in the feedback loop, and PAR-bZIPs in the feed-forward loop, which repress the transcription of the positive elements[12]. More recently, the clock-interacting pacemaker, CIPC was predicted to act as an additional repressor of the CLOCK:CYCLE dimer[19]. However, in contrast to the free-running oscillation demonstrated for *N. vectensis* behavior[6,17,19], transcriptional expression profiles of most candidate genes implicated in the core clock mechanism do not retain their oscillation period in the absence of light[14,15,19].

Here, we employed the CRISPR/Cas9-mediated genome editing system to establish a *Clock* mutant (*Clock*$^{-/-}$) *N. vectensis*. Using behavioral monitoring and transcriptomic analysis, we studied the role of CLOCK in regulating rhythmic locomotor activity and gene expression under various light regimes. The findings show evolutionary conserved roles for CLOCK and suggest that *Clock* has evolved to modulates the ancient hierarchy between light- and circadian clock-regulated physiology and behavior.

Results

Phylogenetic analysis and spatial expression of *Clock* mRNA in *N. vectensis*

Phylogenetic analysis of CLOCK protein sequences showed that it is positioned within the cnidarian branch (Fig.1a). Similar to the protein structure found in other animals, it contains a basic helix–loop–helix (bHLH) DNA binding domain and two Per-Arnt-Sim (PAS) domains[20,21]. PAS domains have been shown as important structural motifs involved in protein-protein interactions that drive the self-sustaining molecular mechanism underlying the circadian clock. To localize *Clock* expression in the cellular and tissue levels, *in situ* hybridization chain reaction (HCRv.3) was performed using probe designed to target the *Clock* mRNA. In WT juvenile four-tentacle stage, low clock expression was observed throughout the animal tissue, and enriched expression was visible in the tentacle endodermis and mesenteries (Fig.1b). This expression pattern resembled the expression observed at late planula stage[22]. Notably, the HCR technique enables to detect low number of transcripts at cellular resolution. Although the expression of *Clock* was low, *Clock* transcripts localized in discrete subcellular regions in the nuclei and soma (Fig.1b). These results characterize the spatial expression of *Clock* with a cellular resolution in the polyp, however, to date, functional manipulation of the *Clock* gene has not been performed in early animal lineages including cnidarians, and its function is unknown in cnidarians[20,21].

Generation of *Clock*$^{-/-}$ *N. vectensis*

To investigate the function of CLOCK, we utilized the CRISPR-Cas9 system to generate a stable *Clock* mutant *N. vectensis*. The CRISPR guide RNA (gRNA), designed to target a region close to the 5`-end of the *Clock* coding sequence (CDS), was synthesized, and microinjected with the endonuclease Cas9 into zygotes (Methods). F0 animals were outcrossed with WT and the F1 progeny were raised to adulthood. Subsequently, F1 animals harboring mutation at the *Clock* locus were identified by genotyping using DNA extracted from bisected physa. We identified 10 different alleles, 6 with a frame-shift mutation including one of 20 bp (*Clock*^{1}), resulting in a premature stop codon (Extended Data Fig. 2). The predicted 203 amino acid truncated protein lacked 459 amino acids including one co-factor dimerization PAS domains (Fig. 1c). To obtain *Clock*$^{-/-}$ homozygous animals, we crossed *Clock1*$^{+/-}$ F1 animals. Genotyping F2 animals

resulted in the expected 25% *Clock*$^{-/-}$ animals. Next, we intercrossed *Clock*$^{-/-}$ animals to obtain F3 *Clock*$^{-/-}$ *N. vectensis* that were used in subsequent experiments, aiming to assess the role of CLOCK in regulating diel behavioral and genetic rhythms.

Clock is necessary to maintain circadian behavior.

Our behavior tracking analysis showed that the locomotor activity of both WT and *Clock*$^{-/-}$ *N. vectensis* has a periodicity of 24h ($p<0.01$) under 12h light: 12h dark (LD) cycles (Fig.1d-d', Supplementary Table 1). Next, to determine whether the *Clock* mutation influences free-running locomotor oscillations, animals were monitored under constant conditions i.e., continuous dark (DD) or continuous light (LL). We discovered that WT animals maintained the rhythmic behavior with a 22h ($p<0.01$) periodicity. In contrast, the locomotor activity of *Clock*$^{-/-}$ *N. vectensis* was arrhythmic (Fig.1e-e' and Fig.1f-f', Supplementary Table 1). To further explore the rhythmicity of *N. vectensis* under LD, we tracked the locomotor activity under a 6h light: 6h dark (LD 6:6) cycle after a 72h entrainment under 12:12 LD. We found that the WT behavior maintained a weak but significant periodicity of 22h ($p<0.01$). Interestingly, the *Clock*$^{-/-}$ *N. vectensis* showed a clear rhythmic behavior with a 12h period ($p<0.01$), pointing towards direct light-dependency (Fig.1g-g'). However, to rule out the effect of a potential endogenous circatidal clock, we entrained the animals under LD 6:6 and tracked their behavior under DD. We found that the WT maintained a free-running periodicity of 22h ($p<0.01$), while the *Clock*$^{-/-}$ *N. vectensis* were arrhythmic (Extended Data Fig.1, Supplementary Table 1).

Clock mutation causes a broad impact on the rhythmic transcriptome.

To investigate the underlying molecular correlate of the arrhythmic behavior phenotype found in *Clock*$^{-/-}$ *N. vectensis*, transcriptional profiling was conducted on WT and *Clock*$^{-/-}$ animals that were sampled in 4h intervals over 24h under LD and DD (Fig.2a). Using the RAIN (rhythmicity analysis incorporating non-parametric methods) algorithm[23], we identified in the WT 2262 genes rhythmic under LD and 2361 rhythmic genes under DD ($p< 0.05$). In *Clock*$^{-/-}$, we detected 1847 rhythmic genes under LD and 1314 under DD (Fig.2b, Extended Data Fig.2, Supplementary Table 2). Overall, we detected 6200/6803 (91.1%) genes with no overlap between genotypes, 3798 (55.8%) genes specific to the WT, and 2402 (35.3%) genes to *Clock*$^{-/-}$ *N. vectensis*, revealing that the *Clock* mutation has a broad impact on the rhythmic transcriptome (Extended Data Fig.2, Supplementary Table 2). To investigate genes strictly under the control of the circadian clock we crossed the two WT gene lists (LD and DD) and obtained 220 genes rhythmic in both LD and DD (Fig.2b, Supplementary Table 3), we refer to them as clock-controlled genes (CCGs). A GO term analysis showed enrichment in regulation of different step of translation, transcription, and mitosis regulation (Fig.2d, Supplementary Table 4) which is coherent with the known function of the *N. vectensis* circadian clock[14]. In *Clock*$^{-/-}$, 188/220 (85%) of the CCGs were not rhythmic under LD nor DD. As such, we have

designated them as *Clock*-dependent CCGs (Fig.2c, Extended Data Fig.2, Supplementary Table 3). Next, we analyzed the *Clock*-dependent CCGs for DNA motif enrichment in their promoter, 1kb upstream of their ATG, and detected a significant enrichment in multiple E-box motif associated with bHLH circadian regulation such as CLOCK, BMAL1, and NPAS2 in 28% of the genes (Fig.2e). Applying the same analytical methods, we discovered that in *Clock*$^{-/-}$ *N. vectensis*, 125 out of 156 genes displayed rhythmic expression patterns under both LD and DD. These genes were arrhythmic in the WT animals (Fig.2c, Extended Data Fig.2 and Supplementary Table 3). As such, we have designated these genes as "neoCCGs". We did not observe any significant enrichment of gene ontology (GO) terms related to circadian rhythms or the presence of circadian E-box motifs in the promoter regions of the neoCCGs. (Fig.2d-e and Supplementary Table 4).

Clock cooperates with light to drive the transcription rhythm of the core clock genes.

Consistent with previous finding in *N. vectensis* [14,15,19], our rhythmic analysis of the eight core clock candidates showed that they are all arrhythmic under DD (Fig.3a and Supplementary Table 2). This finding was also true for the *Clock*$^{-/-}$ *N. vectensis*, however, we observed general altered expression patterns under LD (Fig.3a). Interestingly, *PAR-bZIPc* and *Cry-b* were found to be rhythmic only in WT LD, indicating that light is epistatic on *Clock* (Fig.3a). Notably, the only core clock member included in the *Clock*-dependent CCGs we identified, was *CiPC*, however, its individual expression pattern suggested that it is more likely a dampening factor rather than a true rhythmic clock gene (Fig.3a). Additionally, our analysis revealed that circadian E-box motifs were enriched in most of the core clock genes. (Fig.3b). Given the limitations in using core clock genes mRNA as a true circadian clock marker, we sought to identify new markers that could accurately reflect the circadian rhythm. Through our analysis of the 188 *Clock*-dependent CCGs, we identified 16 genes that displayed rhythmic expression patterns in both our study and a previous study by Leach *et al*. (2019)[14] (Fig.3c, Supplementary Table 5). Among these candidate markers, we selected *Myh7* due to its detectability through both RNA-seq and *in situ* hybridization techniques. Furthermore, the spatial expression pattern of *Myh7* closely resembled that of *Clock*, as evidenced by our analysis (Fig.3d-f).

Clock regulates genetic pathways.

To further evaluate changes in gene expression between the genotypes caused by the *Clock* mutation, differentially expressed gene analysis was performed between genotypes for each light condition. Differentially expressed genes were identified using the Wald test with an adjusted p-value cutoff of 0.05. By analyzing the differentially expressed genes from each light condition, and comparing the genes expressed by all *Clock*$^{-/-}$ samples in comparison with WT samples, we aimed to identify processes regulated by *Clock*. In LD conditions, *Clock*$^{-/-}$ *N. vectensis* showed 457 down-regulated genes and 646 up-regulated

genes, without any significant GO term enrichment (Fig.4a, Supplementary Table 5-6). In DD conditions, *Clock*$^{-/-}$ displayed 2450 down-regulated genes and 1770 up-regulated genes (Fig.4b, Supplementary Table 5). Interestingly, the down-regulated genes showed GO term enrichment in various cellular processes such as spermatid development, mitotic and meiotic cell divisions, and ciliary/flagellar motility. In contrast, we observed that the up-regulated genes were significantly enriched in processes such as the modulation of another organism's processes, sensory perception, and ion transmembrane transport (Fig.4c, Supplementary Table 6).

Discussion

This study offers valuable insights into the evolutionary history of circadian clocks by demonstrating the effects of a loss-of-function *Clock* mutation in the basal metazoan, *Nematostella vectensis*. Through our behavioral assays, we have shown that the *Clock* gene is essential for maintaining rhythmic locomotor activity in the absence of an entraining light cue. These findings suggest that this fundamental aspect of circadian clocks was likely present in the common ancestor of both *N. vectensis* and bilaterian animals, shedding light on the evolution of this critical feature of animal biology. However, our transcriptomic data raises questions regarding the ancestral role of *Clock* in the central clock mechanism and its relationship with the environment.

Studies of homozygous *Clock*$^{-/-}$ flies have shown that *dClock* has a dual role in generating circadian rhythms: as an essential core component of the molecular oscillator and in influencing the direct effects of light on locomotor activity[24,25]. WT flies under standard light-dark cycles anticipate the lights-on and lights-off transitions by slowly increasing activity, while this anticipatory response is obscured in arrhythmic *dClock* mutants[26–28]. In contrast to flies, CLOCK-deficient mice continue to express robust circadian rhythms in locomotor activity, although they do show altered responses to light[29,30]. Overall, these findings suggest that CLOCK has different roles in the generation of circadian rhythms and in modulating responses to light in flies and mice. Interestingly, *Bmal1* is the only known mammalian clock gene whose inactivation results in immediate arrhythmicity at both the behavioral and molecular levels in the absence of external cues[31]. However, since mammalian genes exist as multiple isoforms with partially overlapping functions, it was suggested that functional redundancy may obscure the phenotypic outcome in the case of other clock components, including *mClock*[32–34]. The results presented here are consistent with these previous findings, as observed in the complete loss of rhythmic circadian behavior in *Clock*$^{-/-}$ *N. vectensis* under free-running conditions. However, when exposed to LD cycles, we found that the period of rhythmic behavior in these mutants was light-dependent (Fig.1d-g), indicating that while

the molecular oscillator in *Clock*$^{-/-}$ is disrupted, the light input pathway remains intact. Thus, *Clock* is essential for maintaining circadian behavior in the absence of an entraining cue; however, unlike *dClock*[24,25,28] or *mMop3*[31] (also known as BMAL1), it does not seem to play a functional role in the input pathway as it is not necessary for entraining or generating normal activity levels of behavior to LD cycles.

At the transcriptomic level, previous studies in *N. vectensis* have shown large shifts in the transcriptional profile of many genes after a single day of constant darkness, including the candidate core circadian genes that were found arrhythmic[12,14,22]. Similarly, in our data, the rhythmic expression of these genes, including *Clock*, strongly depends on light-dark cycles while behavior and CCGs are still oscillating in free-running. One explanation for this inconsistency is that using whole animals for sampling material, as in vertebrates[35], has the potential to mask oscillating gene expression signals, particularly if the signals are present in a small number of cells or If tissues have rhythmic gene expression in different phases[10,14]. Another possibility is that the core clock mechanism in cnidarians may differ from that of other animal groups, which could affect the intrinsic transcriptional rhythmicity. However, given the widespread expression pattern of *Clock* mRNA we detected, we chose to perform full animal sampling for our transcriptome analysis (Fig.1b).

Even though LD cycles are the main factor driving rhythmic expression, all eight core clock genes have an altered expression pattern in our *Clock*$^{-/-}$ (Fig.3a). This finding could suggest that *Clock* exerts a fine-tuning regulation on their light-dependent expression. However, while the actual contribution of the transcriptional oscillation of putative core clock genes to the oscillator, if any, remains indefinite, the observation of transcriptomic circadian oscillations and the identification of 125 neoCCGs in *Clock*$^{-/-}$ raises further unexpected questions. The only study describing a similar phenomenon is in liver cells of *Bmal1*$^{-/-}$ mice, which exhibit circadian oscillations at the transcription, translation, and protein phosphorylation levels. The authors proposed that a non-canonical clock driven by ETS factors is functioning[36]. Nevertheless, in our data we did not retrieve any GO term enrichment, suggesting the neoCCGs are not recruited by the oscillator in a coordinated manner. Additionally, we did not identify circadian annotated E-box enrichment within their promoter, nor other binding motif enriched compared to the CCGs which could help identify which factors are responsible for these abnormal oscillations. Although we cannot exclude the possibility of an effect from the predicted truncated CLOCK protein, the rhythmic circadian behavior of the heterozygote *Clock*$^{-/+}$ indicates there is no dominant-negative effect (Extended Data Fig.1). From our results, it is apparent that a functional circadian oscillator persists in the absence of Clock, albeit with altered target genes. It appears that *Clock* is not essential for the core mechanism that drives molecular oscillations. However, the origin of these

oscillations remains unclear, and further research is necessary to elucidate the evolutionary and mechanistic implications of our findings.

Our study revealed that the *Clock*$^{-/-}$ gene exhibits significant differential expression when compared to the WT in LD and DD conditions. Interestingly in DD, the down-regulated genes were mainly involved in cell division and microtubule organization, which suggests a potential function of *Clock* in coordinating cellular processes beyond circadian rhythm. Conversely, the up-regulated genes were linked to sensory perception, indicating a potential novel role of *Clock* in regulating sensory processes. Overall, our findings suggest that *Clock* has non-circadian functions in a light-dependent context in *N. vectensis*, possibly related to developmental processes, as core clock genes are expressed and arrhythmic during planula stages[22]. Our study underscores the need to explore potential novel roles of circadian clock components beyond their established role in regulating the circadian rhythm of adult *N. vectensis*.

Taken as a whole, this study provides novel insights into circadian regulation in *Nematostella vectensis* and sheds light on the evolutionary origin of circadian time maintenance. Our findings indicate that while *Clock* function is conserved from Cnidaria to mammals, it is not a core component of the TTFL. Our findings suggest that the CLOCK protein evolved to alter the light-biological clock hierarchy and facilitate the connection between the core oscillator and the organism, simplifying interactions with the environment. This opens new avenues for investigating cell-type-specific mechanisms of the circadian clock that drive the molecular and phenotypical oscillations of cnidarians. By further exploring the circadian clock mechanisms in cnidarians, we can gain deeper insights into the evolutionary origins of this critical aspect of biology, enhancing our understanding of how organisms have evolved to keep track of time and adapt to their environment.

Methods

Animal husbandry

N. vectensis were grown in 12g.L sea salt water at 17°C, and fed with Artemia *salina nauplii* three times a week. Spawning of gametes and fertilization was performed according to a published protocol[37]. In brief, temperature was raised to 25 °C for 9 h and the animals were exposed to strong white light. Three hours after the induction, oocytes were mixed with sperm to allow fertilization.

CRISPR/Cas9 mediated mutagenesis

Genome editing in *N. vectensis* was carried out following established CRISPR/Cas9 protocols, with slight modifications[38,39]. ZiFiT targeting software (http://zifit.partners.org/)[40] was used to select a guide RNA (gRNA) target site

within the beginning of the *Clock* exon and to design complementary oligonucleotides. To ensure specificity of the gRNA, the selected target site sequence (GGTCCTCTCGTGGACTCTAC) was BLASTed against *Nematostella vectensis* genome (using JGI expected E value threshold of 0.1 to adjust for short sequences; http://genome.jgi.doe.gov/Nemve1/Nemve1.home.html). To generate the gRNA template, the following oligonucleotides were used:

Oligo 1: 5'- TAGGTCCTCTCGTGGACTCTAC -3'

Oligo 2: 5'- AAACGTAGAGTCCACGAGAGGA -3'

To construct the gRNA expression vector, pDR274 (plasmid # 42250; Addgene) was digested with the *BsaI* restriction enzyme. Subsequently, the gRNA oligonucleotides were annealed and cloned into the *BsaI*-digested pDR274 vector. Next, *DraI*-digested gRNA expression vectors, purified via ethanol precipitation followed by PureLink PCR purification kit (Invitrogen), were transcribed and purified using HiScribe T7 High Yield Transcription Kit (New England BioLabs) and illustra Microspin G-50 Columns (GE Healthcare Life Sciences), respectively. Cas9 recombinant protein with nuclear localization signal (260 ng/µl; PNA Bio, USA) was co-injected with the gRNA (140ng/µl) into *N. vectensis* zygotes. Injected embryos were raised in petri dishes at 22°C under constant darkness with daily water changes.

CRISPR/Cas9 mediated mutagenesis screening.

To evaluate genome editing efficiency and mosaicism in F0 animals, genomic DNA flanking the guide sequence was amplified and Sanger sequenced. PCR was performed using two strategies. For the first, PCR reactions were performed using individual injected *N. vectensis* (7-days post-fertilization), directly pipetted into a 25-µl PCR reaction containing a 2x concentration of PCR MasterMix (Tiangen) and 10 pmol of each PCR primer. For the second, genomic DNA was extracted from the physa bisected from live adult animals, after relaxation in 7% $MgCl_2$ (Sigma-Aldrich), using NucleoSpin Tissue DNA purification kit (MACHERY-NAGEL). Subsequent PCR reactions were performed as above using 50-ng of genomic DNA. The primers used for these reactions (listed below) were designed to amplify a ~750bp region around the targeted *Clock* genomic locus. Mosaicism was determined if sequenced PCR products showed overlapping peaks in their chromatograms. The second strategy, which takes advantage of the ability of *N. vectensis* to fully regenerate within a few days[41,42], is the one we refer to in the text hereafter. The injected individuals determined mosaic mutants were raised as F0 founders to sexual maturity and outcrossed with wild-type animals. The progeny of these crosses was raised and individually genotyped as described above. To determine inheritable mutations, sequences were further analyzed using the Tracking of Indels by DEcomposition web-tool (TIDE). TIDE quantifies editing efficiency and identifies the predominant types of DNA insertions and deletions (indel)

mutation composition from a heterogeneous PCR product compared to a wild-type sequence[43]. Different heterozygous mutants were raised to sexual maturity and outcrossed with wild-type animals. The resulting F2 progenies were then raised to sexual maturity and genotyped before spawning for F3. Heterozygous mutants from each F2 progeny were intercrossed to obtain 25% homozygous F3 mutants. All animals used in this study are derived from heterozygous F2 mutants intercrosses, harboring the mutant allele *Clock*^{1}.

PCR genotyping was performed using the following primer:

Forward 5'- GATAAACACGGGCCGAAGATA -3'

Reverse 5'- CAGTCCACGCTGGTCTAAAT -3'

Determination of *Clock*^{1} F3 mutant genotypes

Genomic DNA was extracted as described above and used for following PCR and electrophoresis-based genotyping. PCR primers (listed below) encompassing the *Clock* targeted site were used to produce PCR products of approximately 100 bp. The PCR products were then loaded and migrated by electrophoresis on a 3% Tris-borate-EDTA (TBE) agarose gel supplemented with GelStar Nucleic Acid Gel Stain (Lonza) for approximately one hour. The genotype of each F3 animal was determined by visualizing differences in migration speed of the PCR products caused by the CRISPR/Cas9 genome editing. The homozygous mutant animal (*Clock*$^{-/-}$) produces only the larger ~120 bp amplicon while the wild-type animal (*Clock*$^{+/+}$) produces only the lower ~100 bp amplicon. Animals heterozygous for the deletion (*Clock*$^{+/-}$) produce both the larger mutant and the smaller wild-type amplicons. PCR genotyping was confirmed by subsequent DNA sequencing of selected F3 animals.

PCR was performed using the following primer:

Forward 5'- ACCCCACTGAGTGACCTCTT -3'

Reverse 5'- ATACGCCTGCGCTATACACC -3'

Behavioral assays

Locomotor activity of individual *N. vectensis* were monitored using a lab-made setup equipped with an IP IR camera (Dahua) and a white neon illumination and LD cycles. The camera output 1h mp4 movie files which were AVI converted then stitched. The data collection and analysis were carried out by EthoVision XT8 video tracking software (Noldus information technology, Wageningen, Netherlands). Animals were isolated in wells of six-well plates, each of which was manually defined as a tracking 'arena' in the EthoVision software. Center-point detection with gray scaling (detection range of 25–77,

contour erosion of 1-pixel, high pixel smoothing) was used to monitor movements, which were calculated according to the change in position of the average center pixel each second.

Illumination was provided by a white neon light with an intensity of 17umol. $m^{-2}s^{1}$ (+/−2) and did not significantly affect the experimental temperature (20 °C). The illumination cycles were 12: 12 h LD or 6: 6h LD. Parameters were optimized to ensure that organisms were detected throughout the entire observation period.

Behavior analysis

The total distance moved was summed in hourly bins and individually normalized min/max by the software GraphPad Prism 9.4. The average and standard errors were calculated for all tested animals based on the normalized values of each hour. The oscillation frequencies were evaluated based on the average values of each experiment using Fourier analysis-based software LSP with a $p<0.01$.

RNA-seq experimental design

All polyps were isolated in wells of six-well plates. Then, they were subjected to the 12: 12h LD cycle with 17umol. $m^{-2}s^{1}$ (+/−2) light intensity during 72 hours for entrainment in an incubator with a stable temperature at 18°C. Subsequently, the polyps were divided into 2 experimental subgroups: 12: 12h LD and Continuous Dark or DD. Sampling began at 7 am (ZT0) and was performed at 4-hour intervals over 24 hours. At each time point, three or four individual polyps were sampled from each experimental group, immediately snap-frozen in liquid nitrogen, and transferred to − 80°C for storage.

RNA extraction, library preparation, and sequencing

Total RNA was extracted from all sampled polyps (n = 96) using TRIzol reagent (Invitrogen). Purified RNA samples were analyzed using a NanoDrop 1000 spectrophotometer (Thermo Fisher Scientific) to assess RNA quantity and 2200 TapeStation (Agilent) to assess RNA quality (RNA integrity number, >8.5). From each of the 96 samples (4 biological replicates in LD and 3 in DD, with the highest-quality extracts × 4 experimental subgroups × 7 time points, 1.5 μg of RNA was sent for library preparation (INCPM mRNAseq protocol) and sequencing at the Weizmann Institute Sequencing Unit, Israel. The libraries were sequenced using the bulk MARS-seq protocol (Jaitin et al. Science, 2014, Keren-Shaul et al., Nature Protocols,2019) on an Illumina NovaSeq 6000, resulting in an average of 17 million single-end reads of 113 bases per sample.

Bioinformatic analysis

First, the unique molecular identifier (UMI) sequence of each read was extracted and placed within the read1 header file using UMI-tools extract (umi_tools v1.1). Next, the reads were mapped onto the *N. vectensis* genome (NCBI genome GCA_000209225.1) using STAR (v2.6.0a) (Dobin et al., 2013) with default parameters. Mapped reads were then deduplicated based on UMIs using the umi_tools dedup. The mapped reads were sorted by SAMtools (version 1.9). The number of reads per gene were quantified using HTSeq-Count (v0.12.4) (Anders et al., 2015).

Rhythmicity analysis

Rhythmicity in transcript expression was identified using the RAIN package for R[23]. The RAIN algorithm was run separately for each N. vectensis genotype in each light condition (LD and DD) as one dataset. For each dataset, all replicat es (n=3) for each time point were analyzed as regular time series to detect dai ly oscillating transcripts. We only looked for transcripts with a precise 24-hour period and not a range (e.g., 10 to 14 or 20 to 28 hours). To account for multip le testing, transcript with a Benjamini-Hochberg-corrected RAIN P value < 0.05 were considered confident cyclers. Heatmaps were generated using the heatm ap package (v4.5.5) in R. Venn diagrams were generated using the web tool V enn diagram (http://bioinformatics.psb.ugent.be/webtools/Venn/) And redraw w ith Inkscape. Expression plots were generated using GraphPad Prism (V.9.1).

GO term enrichment analysis

After obtaining the differential gene expression results, Gene Ontology (GO) analysis was performed using the R TopGO package (v2.50.0) to identify the significantly enriched biological processes, cellular components, and molecular functions in the differentially expressed genes. The algorithm assigns a significance score to each GO term based on the enrichment p-value and the specificity of the term. In this study, the GO analysis was performed separately for the up-regulated and down-regulated genes in each condition (LD and DD) to identify the specific biological processes and molecular functions that are affected by the *Clock* mutation.

DNA motif enrichment analysis

DNA motif promoter enrichment analysis was performed using the Homer software (v4.10) and MEME Suite (v5.1.1). First, sequences for promoter regions (1000kb upstream ATG) of differentially expressed genes were extracted. The resulting fasta files were then used as input to the Homer software to identify enriched DNA motifs. Finally, the identified motifs were also analyzed using the MEME Suite to confirm their statistical significance and obtain their corresponding sequence logos. We manually identified in the list of

motif enrichment all the E-box motifs and Circadian E-box motifs. Boxplot were generated using GraphPad Prism version 9.5.1.

Differential Expression Analysis

Differential expression analysis was performed using R (v4.2.2) Bioconductor package, DESeq2 (v1.38.3)[44] . Raw read counts were obtained using I used HTSeq-Count (v0.12.4)[45] and then imported into DESeq2 for normalization and statistical analysis. Differentially expressed genes were identified using the Wald test with an adjusted p-value cutoff of 0.05. The analysis was performed on all the time-points pooled of each genotype per light condition. The output of the analysis includes a list of genes with their log2 fold change, p-value, and adjusted p-value. Volcano-plots were generated using GraphPad Prism version 9.5.1.

HCR v.3 *in situ* hybridization

A custom *Clock* (NVE2080, amplifier: B3 and B5) and *Myh7* probe set (NVE14552, amplifier: B5) were generated. We used *zfHcrt* probe set (ZDB-GENE-040324-1, amplifier: B1 and B3) as a negative control. For HCR on *Nematostella* juvenile, several alterations were made to a previously described protocol[46]. Briefly, polyps were plucked and fixed in 4% PFA overnight at 4°C. Polyps were washed 3× in 1× PBS and then dehydrated and permeabilized with 2×5 min washes in 100% methanol. The samples were stored at –20°C overnight. To rehydrate the samples, a series of graded MeOH/PBST washes were used for 5 min each: 75% MeOH:25% 1× PBST, 50% MeOH:50% 1× PBST, 25% MeOH:75% 1× PBST, and finally 2× washes in 100% 1× PBST. To further permeabilize the polyps, samples were incubated in 10 ug/ml Proteinase K diluted in 1× PBST for 10 min. Samples were quickly washed 3× in 1× PBST, and then post-fixed with 4% PFA for 10 min. After post-fixation, samples underwent 3×5 min washes with 1× 2xSSC+0.1% Triton. From now, the following solutions (Pre-hybridization, hybridization and probe wash buffers) were lab-made from the cnidarian-adapted hybridization buffer[47]. Samples were then pre-hybridized with pre-hybridization buffer at 37°C for 30 min. After pre-hybridization, samples were incubated with 2 pmol of the probe set diluted in hybridization buffer for 16 hr at 37°C. To remove the probe mixture solution, samples were washed 2× for 30 min each with probe wash buffer at 37°C. Samples were washed 2× for 5 min with 5× SSC +0.1% Triton and then treated with probe amplification buffer for 30 min at room temperature. Samples were washed into hairpin amplification buffer containing snap cooled amplifier hairpins and were incubated at room temperature, protected from light, overnight. Samples were then washed with successive 3× 5xSSC +0.1% Triton washes: 2× washes for 15min. Nuclear staining was performed using DAPI 1:1000 in PBST during 1h. Samples were then washed with successive 2×

5xSSC +0.1% Triton washes: 2× washes for 5min. Eventually were slide-mounted in glycerol and stored at 4°C.

Microscopy and Image processing

Samples were imaged using a Zeiss LSM 710 with a x63 oil objective. They were slide-mounted in glycerol. Image manipulation was performed with Fiji[48]. For the double probes *Clock* imaging (Fig1.B), ROIs were generated from each *Clock* probes and only the ROIs positive for the 2 fluorophores were kept. These ROIs were then used to extract from the original picture to select the signal considered as true mRNA signal. Figures were then assembled in Inkscape (http://www.inkscape.org/)

Data availability

The RNA-seq data reported in this study have been deposited to the Sequence Read Archive (SRA), under accession PRJNA935092. All data supporting the findings of this study are included in the manuscript and its supplementary files or available upon request from the corresponding authors.

Acknowledgments

We would like to thank the lab of Yehu Moran (The Hebrew University) for their help with advice on applying the CRISPR-Cas9 system in *Nematostella vectensis*. We thank Ms. Roni Turgeman for her assistance with *N. vectensis* cultures. The research was funded by the Moore Foundation "Unwinding the Circadian Clock in a Sea Anemone" (OL, grant no. 4598), and the Israel Science Foundation (LA, ISF, grant no. 961/19), we also acknowledge German Israeli Foundation GIF Nexus (OL, LA, No. G-1566-413.13/2023). Raphael Aguillon was funded by the Azrieli Foundation. This study represents partial fulfillment of the requirements for a Ph.D. thesis for M. Rinsky at the Faculty of Life Sciences Bar-Ilan University, Israel.

Author Contributions

M.R., R.A., N.S.B., and O.L. designed the research; M.R., R.A., and N.S.B. carried out the experiments; M.R. and R.A. analyzed the data; T.D. performed the bioinformatics; O.L. and L.A. conceived and supervised the project; M.R., R.A., L.A and O.L. wrote the manuscript. All authors read and approved the final manuscript.

No competing Interests

References (typically recommend up to 50)

1. Hut, R. A. & Beersma, D. G. M. Evolution of time-keeping mechanisms: early emergence and adaptation to photoperiod. *Philos. Trans. R. Soc. Lond. B Biol. Sci.* **366**, 2141–2154 (2011).

2. Pittendrigh, C. S. Temporal organization: reflections of a Darwinian clock-watcher. *Annu. Rev. Physiol.* **55**, 16–54 (1993).

3. Quiroga Artigas, G. *et al.* A gonad-expressed opsin mediates light-induced spawning in the jellyfish Clytia. *eLife* **7**, (2018).

4. Taddei-Ferretti, C. & Musio, C. Photobehaviour of Hydra (Cnidaria, Hydrozoa) and correlated mechanisms: a case of extraocular photosensitivity. *J Photochem Photobiol B, Biol* **55**, 88–101 (2000).

5. Gutner-Hoch, E. *et al.* Evidence for rhythmicity pacemaker in the calcification process of scleractinian coral. *Sci. Rep.* **6**, 20191 (2016).

6. Oren, M. *et al.* Profiling molecular and behavioral circadian rhythms in the non-symbiotic sea anemone Nematostella vectensis. *Sci. Rep.* **5**, 11418 (2015).

7. Hoadley, K. D., Szmant, A. M. & Pyott, S. J. Circadian clock gene expression in the coral Favia fragum over diel and lunar reproductive cycles. *PLoS ONE* **6**, e19755 (2011).

8. Sorek, M. *et al.* Setting the pace: host rhythmic behaviour and gene expression patterns in the facultatively symbiotic cnidarian Aiptasia are determined largely by Symbiodinium. *Microbiome* **6**, 83 (2018).

9. Levy, O. *et al.* Light-responsive cryptochromes from a simple multicellular animal, the coral Acropora millepora. *Science* **318**, 467–470 (2007).

10. *The cnidaria, past, present and future*. (Springer International Publishing, 2016). doi:10.1007/978-3-319-31305-4.

11. Reitzel, A. M., Tarrant, A. M. & Levy, O. Circadian clocks in the cnidaria: environmental entrainment, molecular regulation, and organismal outputs. *Integr. Comp. Biol.* **53**, 118–130 (2013).

12. Reitzel, A. M., Behrendt, L. & Tarrant, A. M. Light entrained rhythmic gene expression in the sea anemone Nematostella vectensis: the evolution of the animal circadian clock. *PLoS ONE* **5**, e12805 (2010).

13. Shoguchi, E., Tanaka, M., Shinzato, C., Kawashima, T. & Satoh, N. A genome-wide survey of photoreceptor and circadian genes in the coral, Acropora digitifera. *Gene* **515**, 426–431 (2013).

14. Leach, W. B. & Reitzel, A. M. Transcriptional remodelling upon light removal in a model cnidarian: Losses and gains in gene expression. *Mol. Ecol.* **28**, 3413–3426 (2019).

15. Leach, W. B., Macrander, J., Peres, R. & Reitzel, A. M. Transcriptome-wide analysis of differential gene expression in response to light:dark cycles in a model cnidarian. *Comp. Biochem. Physiol. Part D Genomics Proteomics* **26**, 40–49 (2018).

16. Rinsky, M. *et al.* Temporal gene expression patterns in the coral Euphyllia paradivisa reveal the complexity of biological clocks in the cnidarian-algal symbiosis. *Sci. Adv.* **8**, eabo6467 (2022).

17. Hendricks, W. D., Byrum, C. A. & Meyer-Bernstein, E. L. Characterization of circadian behavior in the starlet sea anemone, Nematostella vectensis. *PLoS ONE* **7**, e46843 (2012).

18. Tarrant, A. M., Helm, R. R., Levy, O. & Rivera, H. E. Environmental entrainment demonstrates natural circadian rhythmicity in the cnidarian Nematostella vectensis. *J. Exp. Biol.* **222**, (2019).

19. Leach, W. B. & Reitzel, A. M. Decoupling behavioral and transcriptional responses to color in an eyeless cnidarian. *BMC Genomics* **21**, 361 (2020).

20. Hennig, S. *et al.* Structural and functional analyses of PAS domain interactions of the clock proteins Drosophila PERIOD and mouse PERIOD2. *PLoS Biol.* **7**, e94 (2009).

21. Shearman, L. P. *et al.* Interacting molecular loops in the mammalian circadian clock. *Science* **288**, 1013–1019 (2000).

22. Peres, R. *et al.* Developmental and light-entrained expression of melatonin and its relationship to the circadian clock in the sea anemone Nematostella vectensis. *Evodevo* **5**, 26 (2014).

23. Thaben, P. F. & Westermark, P. O. Detecting rhythms in time series with RAIN. *J. Biol. Rhythms* **29**, 391–400 (2014).

24. Allada, R., Kadener, S., Nandakumar, N. & Rosbash, M. A recessive mutant of Drosophila Clock reveals a role in circadian rhythm amplitude. *EMBO J.* **22**, 3367–3375 (2003).

25. Kim, E. Y. *et al.* Drosophila CLOCK protein is under posttranscriptional control and influences light-induced activity. *Neuron* **34**, 69–81 (2002).

26. Sehgal, A., Price, J. L., Man, B. & Young, M. W. Loss of circadian behavioral rhythms and per RNA oscillations in the Drosophila mutant timeless. *Science* **263**, 1603–1606 (1994).

27. Lee, C., Bae, K. & Edery, I. The Drosophila CLOCK protein undergoes daily rhythms in abundance, phosphorylation, and interactions with the PER-TIM complex. *Neuron* **21**, 857–867 (1998).

28. Allada, R., White, N. E., So, W. V., Hall, J. C. & Rosbash, M. A mutant Drosophila homolog of mammalian Clock disrupts circadian rhythms and transcription of period and timeless. *Cell* **93**, 791–804 (1998).

29. Debruyne, J. P. *et al.* A clock shock: mouse CLOCK is not required for circadian oscillator function. *Neuron* **50**, 465–477 (2006).

30. Vitaterna, M. H. *et al.* Mutagenesis and mapping of a mouse gene, Clock, essential for circadian behavior. *Science* **264**, 719–725 (1994).

31. Bunger, M. K. *et al.* Mop3 is an essential component of the master circadian pacemaker in mammals. *Cell* **103**, 1009–1017 (2000).

32. Selby, C. P., Thompson, C., Schmitz, T. M., Van Gelder, R. N. & Sancar, A. Functional redundancy of cryptochromes and classical

photoreceptors for nonvisual ocular photoreception in mice. *Proc Natl Acad Sci USA* **97**, 14697–14702 (2000).

33. Reppert, S. M. & Weaver, D. R. Coordination of circadian timing in mammals. *Nature* **418**, 935–941 (2002).

34. Asher, G. & Schibler, U. A CLOCK-less clock. *Trends Cell Biol.* **16**, 547–549 (2006).

35. Albrecht, U. Timing to perfection: the biology of central and peripheral circadian clocks. *Neuron* **74**, 246–260 (2012).

36. Ray, S. *et al.* Circadian rhythms in the absence of the clock gene Bmal1. *Science* **367**, 800–806 (2020).

37. Genikhovich, G. & Technau, U. Induction of spawning in the starlet sea anemone Nematostella vectensis, in vitro fertilization of gametes, and dejellying of zygotes. *Cold Spring Harb. Protoc.* **2009**, pdb.prot5281 (2009).

38. Hwang, W. Y. *et al.* Efficient genome editing in zebrafish using a CRISPR-Cas system. *Nat. Biotechnol.* **31**, 227–229 (2013).

39. Ikmi, A., McKinney, S. A., Delventhal, K. M. & Gibson, M. C. TALEN and CRISPR/Cas9-mediated genome editing in the early-branching metazoan Nematostella vectensis. *Nat. Commun.* **5**, 5486 (2014).

40. Sander, J. D. *et al.* ZiFiT (Zinc Finger Targeter): an updated zinc finger engineering tool. *Nucleic Acids Res.* **38**, W462-8 (2010).

41. Reitzel, A. M., Burton, P. M., Krone, C. & Finnerty, J. R. Comparison of developmental trajectories in the starlet sea anemone Nematostella vectensis: embryogenesis, regeneration, and two forms of asexual fission. *Invertebr. Biol.* **126**, 99–112 (2007).

42. Burton, P. M. & Finnerty, J. R. Conserved and novel gene expression between regeneration and asexual fission in Nematostella vectensis. *Dev. Genes Evol.* **219**, 79–87 (2009).

43. Brinkman, E. K., Chen, T., Amendola, M. & van Steensel, B. Easy quantitative assessment of genome editing by sequence trace decomposition. *Nucleic Acids Res.* **42**, e168 (2014).

44. Love, M. I., Huber, W. & Anders, S. Moderated estimation of fold change and dispersion for RNA-seq data with DESeq2. *Genome Biol.* **15**, 550 (2014).

45. Anders, S., Pyl, P. T. & Huber, W. HTSeq — a Python framework to work with high-throughput sequencing data. *Bioinformatics* **31**, 166–169 (2015).

46. Choi, H. M. T. *et al.* Third-generation in situ hybridization chain reaction: multiplexed, quantitative, sensitive, versatile, robust. *Development* **145**, (2018).

47. Sinigaglia, C., Thiel, D., Hejnol, A., Houliston, E. & Leclère, L. A safer, urea-based in situ hybridization method improves detection of gene expression in diverse animal species. *Dev. Biol.* **434**, 15–23 (2018).

48. Schindelin, J. *et al.* Fiji: an open-source platform for biological-image analysis. *Nat. Methods* **9**, 676–682 (2012).

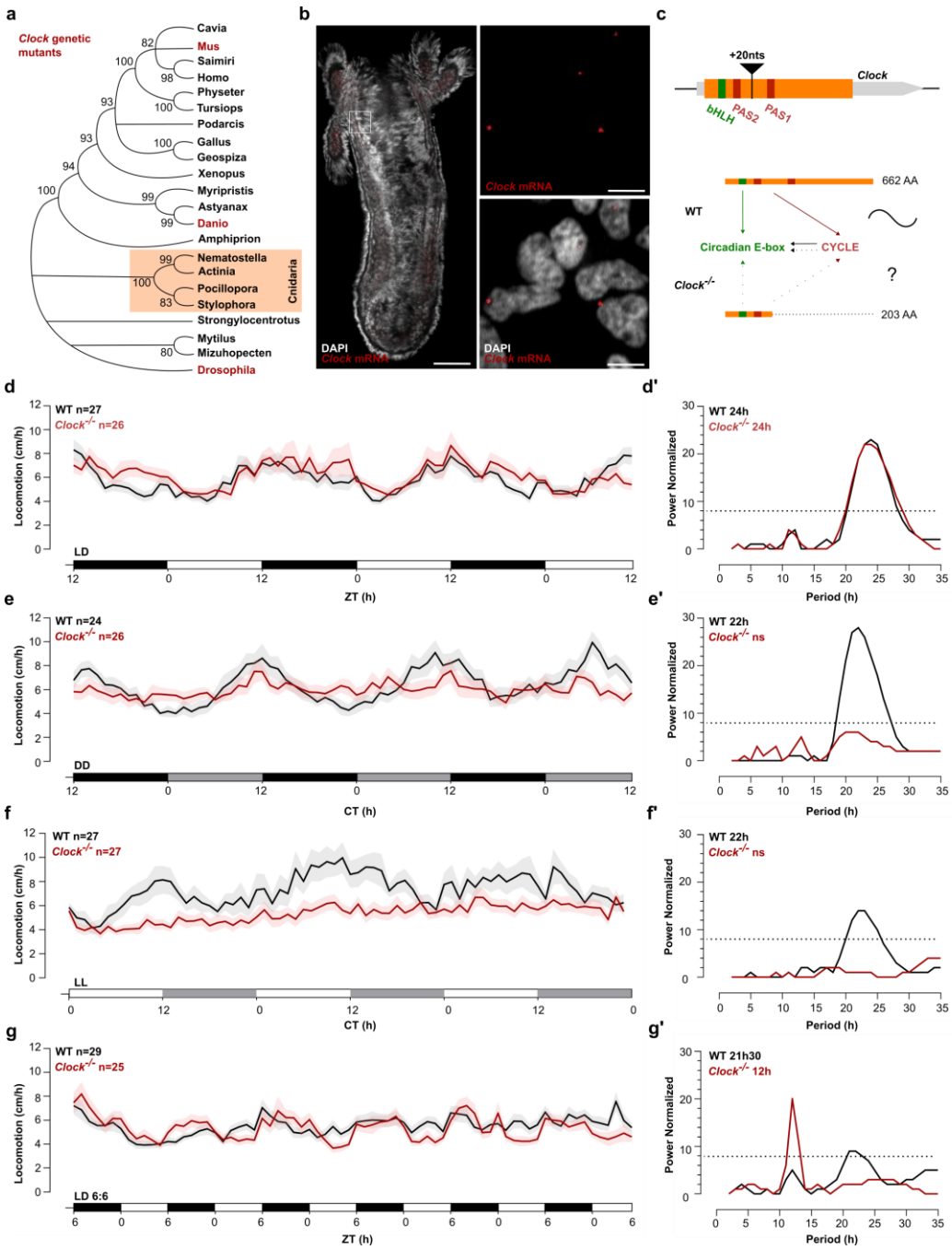

Fig.1 *Clock* is necessary to maintain circadian behavior.

(**A**) Phylogenetic tree showing the evolutionary relationship of CLOCK orthologs across different animal species. (**B**) *In situ* hybridization of *Clock* in the WT juvenile with scale bars representing 0.1mm and 5µm. (**C**) Schematic representation of the *Clock* gene in grey, with the open reading frame (ORF) in orange and the conserved protein domains bHLH (green) and PAS1 and PAS2 (dark red). The CRISPR generated allele has a 20nt insertion after the PAS1 domain, represented by a black arrowhead. (**D-G**) Normalized locomotor activity (a.u), hourly binned over 72h, under different light conditions: 12h light:12h dark, continuous dark, continuous light, and 6h light:6h dark. The black line represents the WT and the red line represents the *Clock*$^{-/-}$ mutant. (**D'-G'**) Periodograms for each corresponding light condition. The significant period value ($p<0.01$) is indicated for each genotype in the top left corner of each graph.

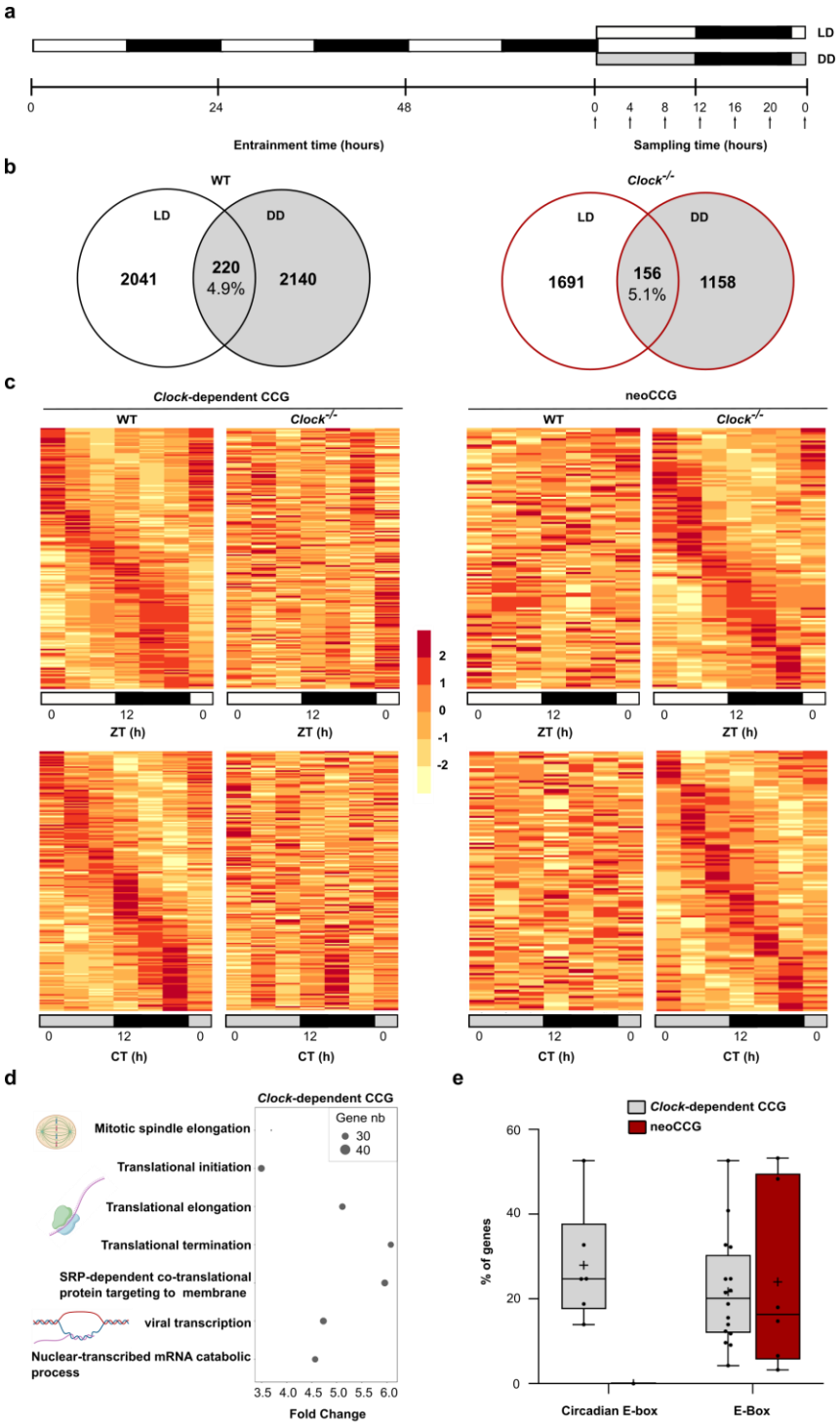

Fig.2 *Clock* mutation causes a broad impact on the rhythmic transcriptome.

(**A**) Overview of the experimental design used to generate RNA-seq data. Polyps were entrained for 72 hours before sampling at 4-hour intervals over a 24-hour period (dark arrows) in both LD and DD cycles. (**B**) Venn diagram comparing the total number of rhythmic genes identified in WT and *Clock*$^{-/-}$ in LD and DD cycles. (**C**) Heatmap showing genotype-specific rhythmic transcripts in WT and *Clock*$^{-/-}$. (**D**) Gene Ontology (GO) terms that were significantly enriched (Bonferroni corrected $p < 0.05$) for rhythmic genes in WT. (**E**) De novo sequence motif analysis of circadian transcriptional regulators detected in WT and *Clock*$^{-/-}$ using Homer/MEME. The 1000bp upstream ATG of each rhythmic gene was used for motif analysis.

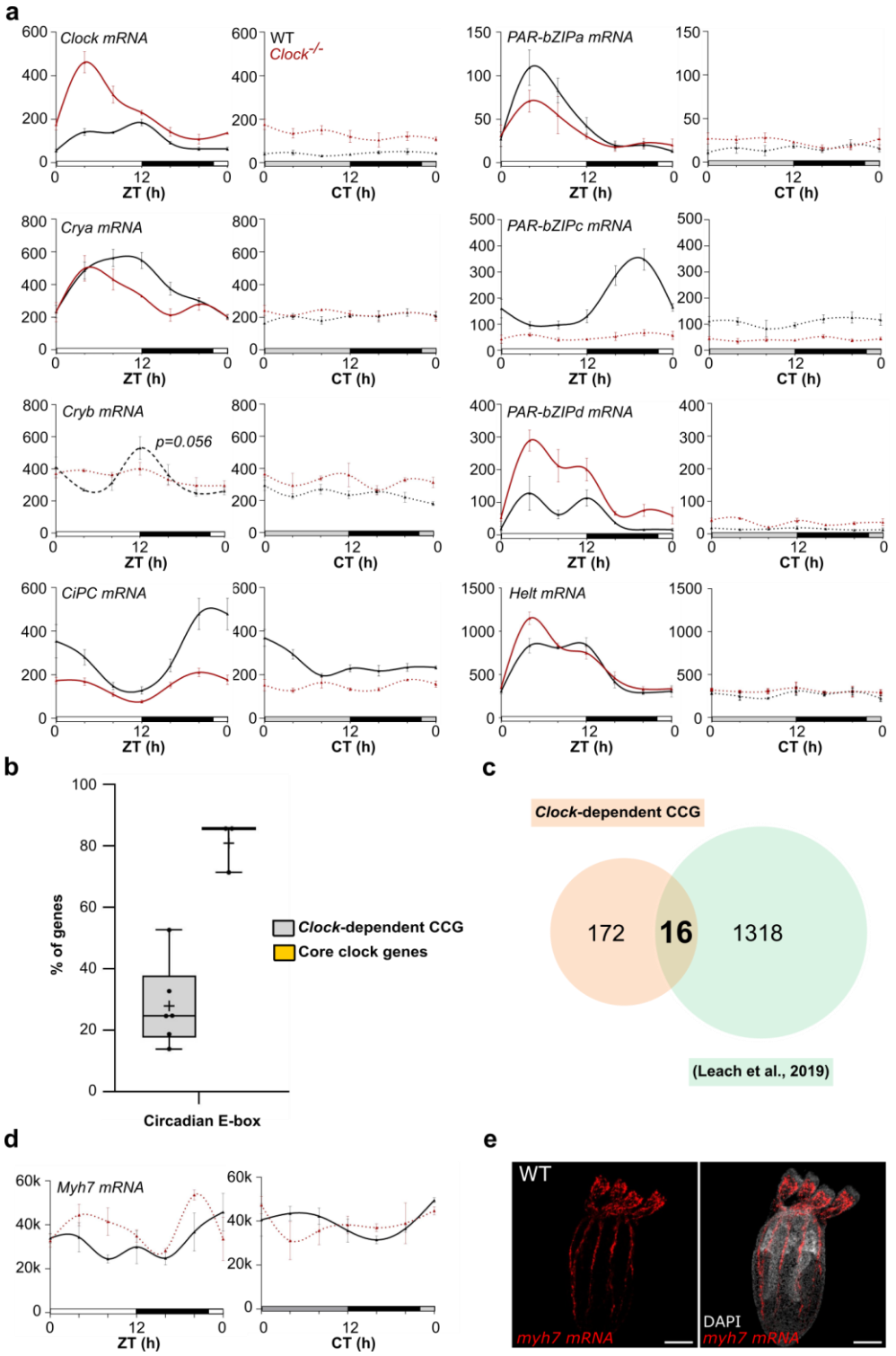

Fig.3 *Clock* cooperates with light to drive the transcription rhythm of the core clock genes.

(**A**) Each core clock gene is individually plotted showing the read count over 24h in LD and DD in WT (black) and *Clock*$^{-/-}$ (red). The continuous line represents significant rhythmicity (RAIN $p<0.05$) while the dashed line indicates no rhythmicity. (**B**) The presence of Circadian E-box in all core clock gene promoters was detected using HOMER within 1000bp upstream ATG. (**C**) Conserved rhythmic genes were selected from our WT data and Leach *et al*., 2020. (**D**) The temporal expression pattern of Clock-downstream gene *Myh7* is shown. (**E**) *In situ* hybridization of *Myh7* in the WT juvenile with scale bars representing 0.1mm. Nuclei are DAPI-stained, colored in grey.

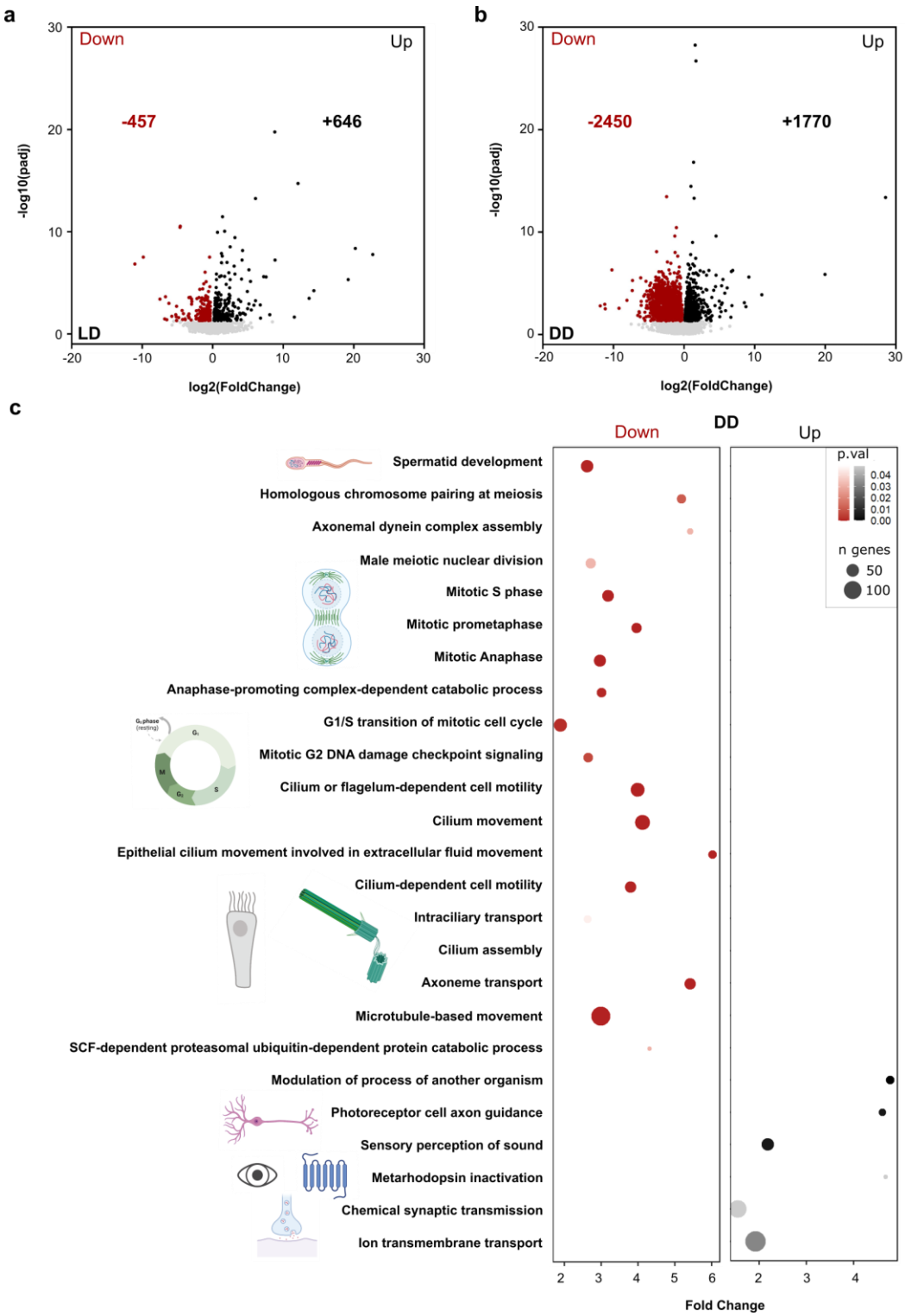

Fig.4 *Clock* regulates genetic pathways.

(**A**) Volcano plot showing the differential expression of genes between WT and *Clock*$^{-/-}$ in LD. The dashed lines indicate the threshold used to detect DEGs (Padj<0.05) and the WT and *Clock*$^{-/-}$ are represented by black and red dots, respectively. (**B**) Volcano plot showing the differential expression of genes between WT and *Clock*$^{-/-}$ in DD (**C**) Gene Ontology (GO) terms with significant fold-enrichment (Bonferroni corrected p-value < 0.05) are shown for DEG analysis in DD.

Extended Data Fig.1 Generation of *Clock* mutant by CRISPR-Cas9-mediated mutagenesis.

Nucleotide and translated amino acid sequences of wild-type and mutant alleles. sgRNA target site is boxed in green, and PAM site are shown in green. Predicted translation termination site is boxed in black. Insertion is labeled in red. Predicted immature peptide sequences in red.

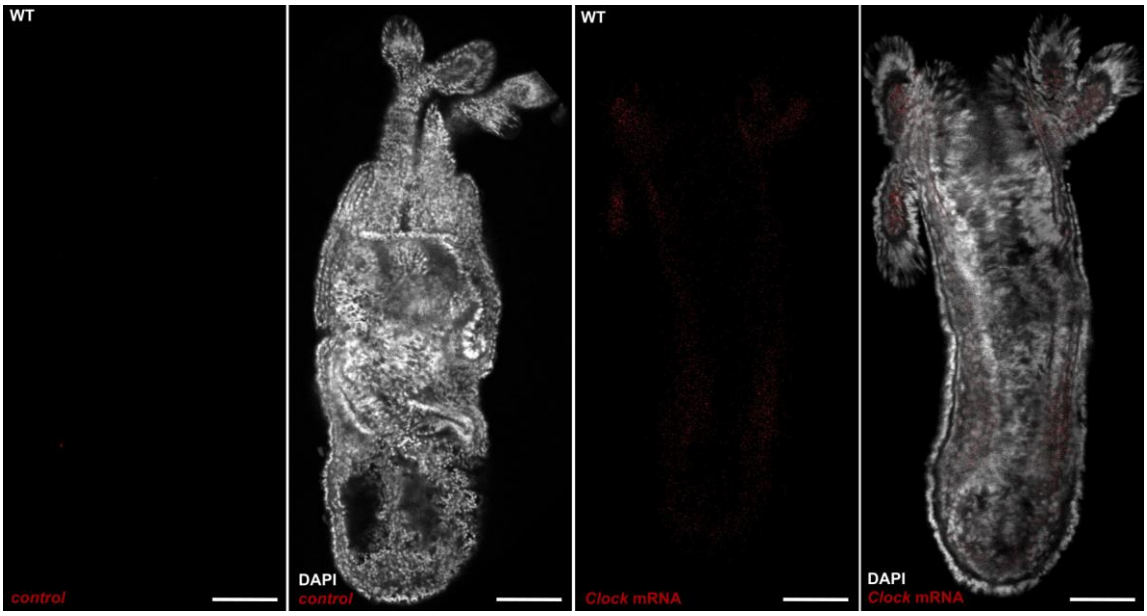

Extended Data Fig.2 Spatial expression pattern of *Clock* reveals endodermis enrichment.

Max projection of *N. vectensis* at 4 tentacle stages, showing signal in Red from the two-channel (*Clock*-B1/*Clock*-B3 for *Clock* mRNA detection and *Clock*-B1/*zfHcrt*-B3 for the control) redundant detection. Nuclei are labeled with DAPI. Scale bar: 0.1 mm .

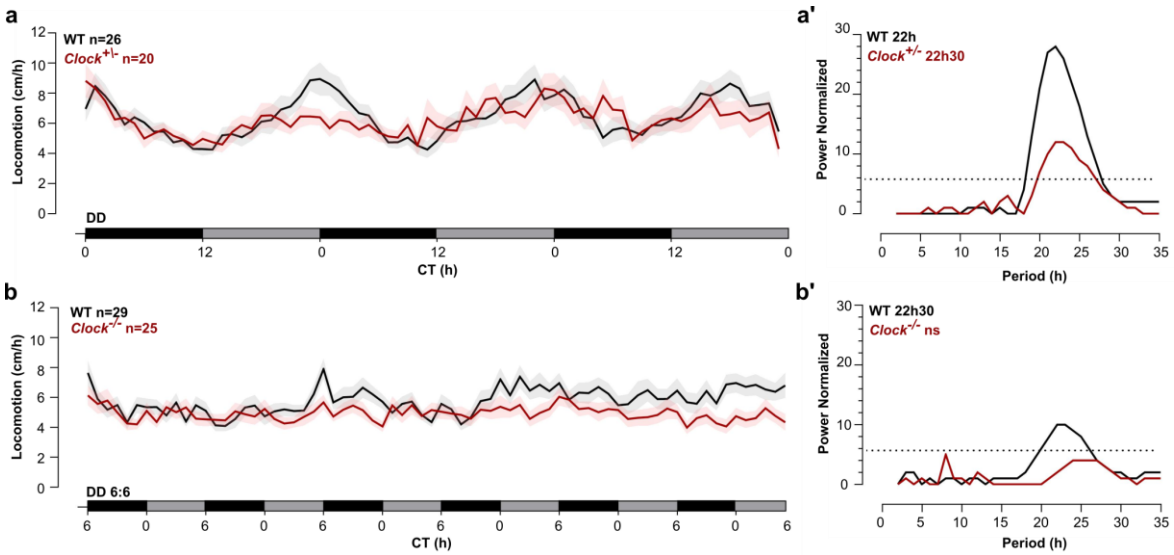

Extended Data Fig.3 *Clock* is necessary to maintain circadian behavior.

(**A-B**) Normalized locomotor activity (a.u), hourly binned over 72h, in continuous dark. The black line represents the WT, and the red line represents the *Clock*$^{-/+}$. (**A'-B'**) Periodograms for each corresponding light condition. The significant period value ($p<0.01$) is indicated for each genotype in the top left corner of each graph.

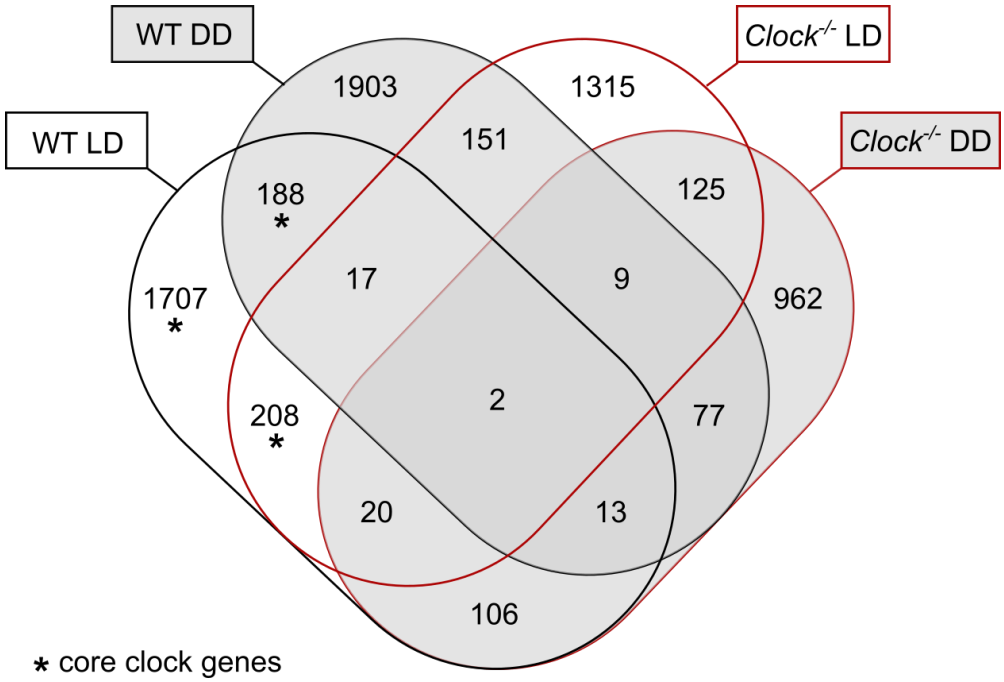

Extended Data Fig.4 *Clock* causes a broad impact on the rhythmic transcriptome.

Venn diagram showing the overlap and unique sets of rhythmic genes identified in wild-type (WT) and *Clock*$^{-/-}$ mutant under light-dark (LD) and constant darkness (DD) conditions. The asterisk (*) indicates the core circadian genes that exhibit rhythmic expression in both WT and *Clock*$^{-/-}$ in both LD and DD conditions.